

Effect of Cu-Dopant on the Structural, Magnetic and Electrical Properties of ZnO

D Aryanto¹, C Kurniawan¹, A Subhan¹, T Sudiro¹, P Sebayang¹, M Ginting¹, S M K Siregar² and Nasruddin M N²

¹Research Center for Physics, Indonesian Institute of Sciences, Serpong 15314, Tangerang Selatan, Banten, Indonesia

²Postgraduate Program, Universitas Sumatera Utara, Medan 20155, Indonesia

Email: masno.ginting@gmail.com

Abstract. Zn_{1-x}Cu_xO ($x = 0, 2, 3$, and 4 at.%) was synthesized by using solid-state reaction technique. The ZnO and CuO powders were mixed and then milled by using high-speed shaker mill. The influence of Cu dopants on the structure, magnetic, and electrical properties was investigated by using XRD, VSM, and I - V and C - V measurements. The XRD analysis showed that the Zn_{1-x}Cu_xO had hexagonal wurtzite polycrystalline. The diffraction intensity decreased and the peak position shifted directly to a higher 2θ angle with increasing the dopant concentration. Furthermore, the lattice parameters decreased when the ZnO was doped with $x = 0.04$, which indicated that the crystal structure changed. The increase of Cu dopants was believed to affect the magnetic and electrical properties of ZnO.

Keywords: ZnO, structural, magnetic, electrical properties, and Cu-dopant

1. Introduction

ZnO is a semiconductor which has a band gap energy, E_g , of 3.37 eV. It was potentially used for some applications such as solar energy conversion, storage, spintronics, gas sensing, optoelectronics, photovoltaic, varistors, photocatalysts, piezoelectric devices, LED, UV light emitters, luminescent devices, field emission electron sources and nanoscale power generator [1-4]. ZnO doped with transition metals of Mn, Fe, Co and Ni shows a ferromagnetic behavior which makes ZnO as a strong candidate in the realization of spintronics [5,6]. The ferromagnetic properties of ZnO at room temperature due to transition metal dopants have widely been investigated [7]. Cu, which is one of the dopant materials to ZnO, is intensively studied as a potential alternative material for DMS (Dilute Magnetic Semiconductor) [8]. The study by Owens [7] showed that Cu-doped ZnO has a ferromagnetic behavior at above room temperature. Various methods were used to synthesize Cu-doped ZnO, such as solid state reaction [4,9] coprecipitation [1,10], and citrate sol-gel [11,4].

Zheng *et al.* [6] showed theoretically and experimentally that ZnO with a variation of Cu-dopant concentrations has ferromagnetic properties at room temperature. Another study by Karamat *et al.* [12] showed that ZnO thin film doped with 1-3 at.% Cu was ferromagnetic whereas when doped with 5 at.% Cu it had diamagnetic behavior. Cu-doped ZnO nanoparticles synthesized through sol-gel method and annealed at N₂, O₂, and Ar environments have wurtzite hexagonal structure and ferromagnetic behavior [4,13,14]. Iqbal *et al.* [15] and Yildirim & Durucan [16] have successfully substituted Cu ions to ZnO matrix by using the co-precipitation method so that Cu-doped ZnO became ferromagnetic.



However, only a few studies which reported the synthesis of ZnO-based DMS material by using solid state reaction method. The advantages of solid state reaction compared with the other methods such as ion implantation and thin film deposition is a relative simple, cheap, and easily scaled-up [7]. This paper reports the syntheses of Cu-doped ZnO by using solid state reaction method. The effects of varying doping composition to the structures, electrical and magnetic properties were studied by using XRD, *I-V* meter, *C-V* meter, and VSM will also be discussed.

2. Experimental Method

2.1 Syntheses of $\text{Zn}_{1-x}\text{Cu}_x\text{O}$

Syntheses of $\text{Zn}_{1-x}\text{Cu}_x\text{O}$ ($x = 0, 2, 3$, and 4 at.%) was done through the solid state reaction. ZnO and CuO powders were utilized as starting materials. They were mixed and milled in the cylindrical stainless steel vial with stainless steel balls. The ratio of the mixed powder and balls was 1: 10. The process was done by wet milling for 3 hours with toluene as solvent. Afterward, the milled powder was dried in an oven at 100°C for 3 hours. The dried, milled powder was then pressed into bulk with 15 mm in diameter and 2 mm in thickness by using an automatic axial hydraulic press with 1500 kgf/cm^2 in load. All bulk samples were finally sintered at 900°C for 8 hours in the air with a heating rate of 10°C/min .

2.2 Characterization

The phase and crystal parameters of all samples were identified by XRD (Rigaku, SmartLab) using $\text{Cu K}\alpha$ radiation ($\lambda = 1.5406\text{ \AA}$). *I-V* meter (Fluke, 8842A multimeter high impedance) and *C-V* meter (Keithley, 590 CV Analyzer) were used to analyze their electrical properties. The magnetic properties were measured by using Vibrating Sample Magnetometer (VSM 250, Dexion Magnet).

3. Results and Discussion

Figure 1(a) shows the XRD patterns of the bulk samples of $\text{Zn}_{1-x}\text{Cu}_x\text{O}$ ($x = 0, 2, 3$ and 4 at.%) synthesized by using the solid state reaction. The lattice planes at the 2θ angle of $31.77^\circ, 32.68^\circ, 34.2^\circ, 36.26^\circ, 47.54^\circ, 56.59^\circ, 62.85^\circ, 66.37^\circ, 67.95^\circ, 69.08^\circ, 72.55^\circ, 76.96^\circ, 81.37^\circ$ and 89° were (100), (002), (101), (102), (110), (103), (200), (112), (201), (103), (202), (004), (202), (104) and (203), respectively. The results indicated that all samples were polycrystalline with wurtzite hexagonal structure. The Cu-doped samples showed tenorite (CuO) peaks at the 2θ angle around $32.63^\circ, 35.62^\circ$ and 38.80° (see Figure 1.(b)). The XRD patterns also revealed the FWHM of (002) plane becoming wider when ZnO was doped with 2-3 at.% Cu (Figure1.(c)). However, the FWHM became narrow when ZnO was doped with 4 at.% Cu. Furthermore, the (002) plane shifted to a higher 2θ angle. It is believed that Cu^{2+} ions have substituted Zn^{2+} on the ZnO lattice [17, 18, 19]. However, some amount of CuO did not react with ZnO which was indicated by the presence of CuO on the XRD patterns. From XRD analysis there was no indication that the secondary phases such as Cu_5Zn_8 or CuZn were formed [7].

The crystal parameters, such as lattice constant, lattice parameter ratio, *d*-spacing and crystal size could then be determined. The lattice parameters (*a* and *c*) from hexagonal phase were determined from (100) and (002) planes by using the following equations.

$$a = \frac{\lambda}{\sqrt{3} \sin \theta} \sqrt{h^2 + hk + k^2} \quad (1)$$

and

$$c = \frac{\lambda}{2 \sin \theta} l \quad (2)$$

where λ is the wavelength, θ is the Bragg's angle of diffraction peak (002), and $h k l$ are the Miller indices. The obtained crystal parameters are given in Table 1. The values of *a* and *c* obtained at

present were smaller compared with the those of theory (JCPDS No. 00-005-0664) where the point a is 3.249 Å and c is 5.205 Å. These results indicated that, partly, Cu^{2+} ions substituted Zn^{2+} ions. The ionic radius of Zn^{2+} (0.60 Å) which was greater than that of Cu^{2+} (0.57 Å) was believed to contribute to the changes in the lattice parameters. The ratio c/a of $\text{Zn}_{1-x}\text{Cu}_x\text{O}$ samples was constant, which means that the dopants have mostly done the substitution [20].

The crystallite size was calculated by using Equation (3).

$$D = \frac{0.9 \lambda}{\beta \cos \theta} \quad (3)$$

where β is the FWHM of the diffraction peak of (002). The crystal sizes of all samples were in the range of 49.9 to 50.9 nm.

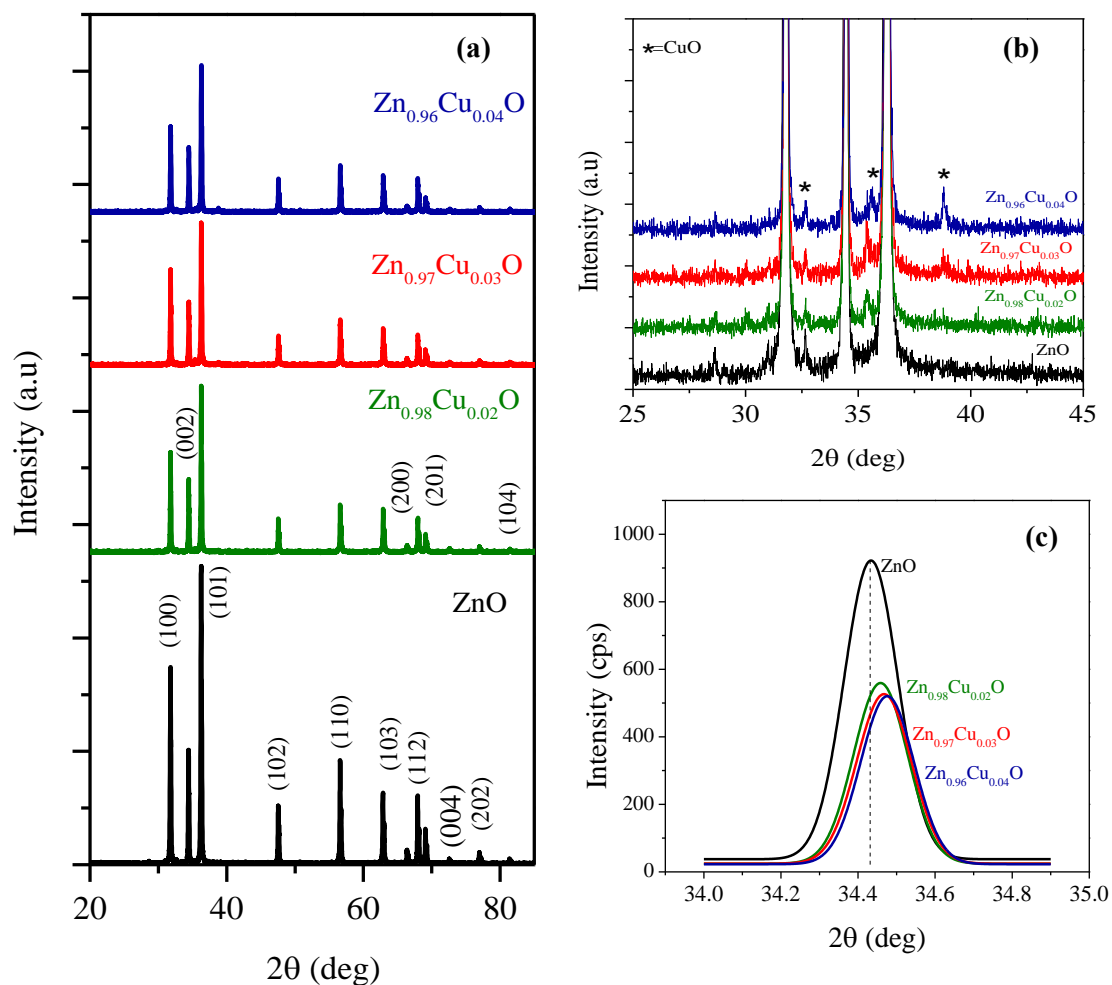


Figure 1. (a) The XRD patterns of $\text{Zn}_{1-x}\text{Cu}_x\text{O}$ ($x = 0, 2, 3$ and 4 at%), (b) Detail observations on 2θ of 25° to 45° and (c) plane peak of (002)

Figure 2 shows the current (I)-voltage (V) properties of $\text{Zn}_{1-x}\text{Cu}_x\text{O}$ ($x = 0, 2, 3$ and 4 at.%) measured at the atmospheric environment and room temperature. The measurement results showed the almost linear relationship between current and voltage for all samples. The calculated resistivity (ρ) and conductivity (σ) are given in Table 2. Based on the calculated results, the conductivity increased with

increasing Cu dopant. This phenomenon can be explained by noting that some amount of Cu^{2+} ions having substituted Zn^{2+} ions on the ZnO lattice increased with the increase in dopant concentration. Cu has greater conductivity than Zn, where the Cu conductivity is $58.5 \times 10^6 \text{ S/m}$ [21] and Zn is $16.6 \times 10^6 \text{ S/m}$ [22]. The measured conductivities of all samples were around of $2.159 \times 10^{-8} \text{ S/cm}$ to $2.624 \times 10^{-8} \text{ S/cm}$. Table 2 also shows the measured dielectric constant (ϵ_r). The dielectric constant changed due to the addition of dopant concentration. It was believed that the changes in dielectric constant value were due to the crystal defects on the bulk of $\text{Zn}_{1-x}\text{Cu}_x\text{O}$ as the effect of Cu^{2+} ions substituting ions at the ZnO crystal. The strain happening due to dopant effect caused dislocation defects on grain boundaries [23]. Besides, the presence of CuO phase in $\text{Zn}_{1-x}\text{Cu}_x\text{O}$ bulk was also believed to cause the presence of crystal defect. This case was confirmed by XRD patterns in Figure 1.

Table 1. The calculated lattice parameters a , c , c/a and the crystallite size (D) of $\text{Zn}_{1-x}\text{Cu}_x\text{O}$ ($x=0, 2, 3$ and 4 at.%) samples on the (002) plane

$\text{Zn}_{1-x}\text{Cu}_x\text{O}$ (at.%) Sample	a (Å)	c (Å)	c/a	FWHM (deg)	D (nm)
$x=0$	3.249	5.205	1.602	0.154	50.6
$x=2$	3.248	5.201	1.601	0.151	50.5
$x=3$	3.248	5.200	1.601	0.154	49.9
$x=4$	3.247	5.199	1.601	0.150	50.9

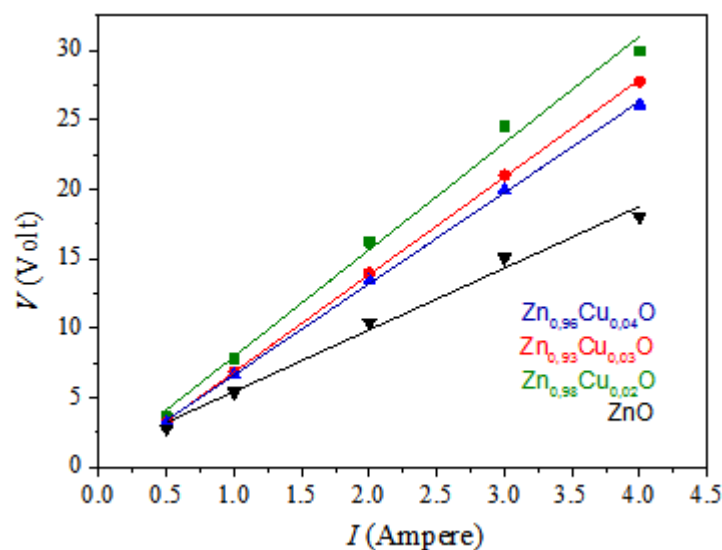


Figure 2. I - V curve of $\text{Zn}_{1-x}\text{Cu}_x\text{O}$

Table 2. The electrical properties of $\text{Zn}_{1-x}\text{Cu}_x\text{O}$ samples

Sample $\text{Zn}_{1-x}\text{Cu}_x\text{O}$ (at%)	ρ (Ωcm)	σ (S/cm)	ϵ_r
$x=0$	3.259×10^7	3.068×10^{-8}	12.52
$x=2$	4.631×10^7	2.159×10^{-8}	14.87
$x=3$	4.279×10^7	2.337×10^{-8}	14.14
$x=4$	3.812×10^7	2.624×10^{-8}	15.92

Figure 3 shows the hysteresis curve of $\text{Zn}_{1-x}\text{Cu}_x\text{O}$ ($x=0, 2, 3$ and 4 at%) samples at room temperature below 20 kOe. It can be seen that the ZnO powder without heat treatment behaved as a diamagnetic (the black line in Figure 3.(a)). This phenomenon means that undoped ZnO powder used

in this research is diamagnetic material [24]. ZnO became paramagnetic if the number of dopants was increased (Figure 3.(a)). The detailed observation on hysteresis curve for ZnO doped with 2 at.% Cu showed the minor effect of diamagnetic behavior up to 20 kOe (Figure 3.(b)). Increasing the concentration of Cu to be 3 at.% caused the minor diamagnetic effect observed up to 14 kOe (Figure 3.(c)). Meanwhile, the addition of 4 at.% Cu dopant caused the magnetic property changed from diamagnetic to paramagnetic (Figure 3.(d)). The change in magnetic property was influenced by CuO phase for Cu-doped ZnO (as shown in the XRD patterns). In this research, the source of doping was obtained from CuO. However, the presence of CuO in the sample did not cause ferromagnetism because it behaves as paramagnetic above 250 K [7]. However, the present result supported the previous report of Hsu *et al.* [17], where the addition of 1.93 and 3.01 at.% Cu on ZnO produced the paramagnetic material. Likewise, Vachhani *et al.* [25] showed that, in general, Cu-doped ZnO sintered at high temperature becomes paramagnetic. This case could be due to the CuO phase formed at the higher sintering temperature.

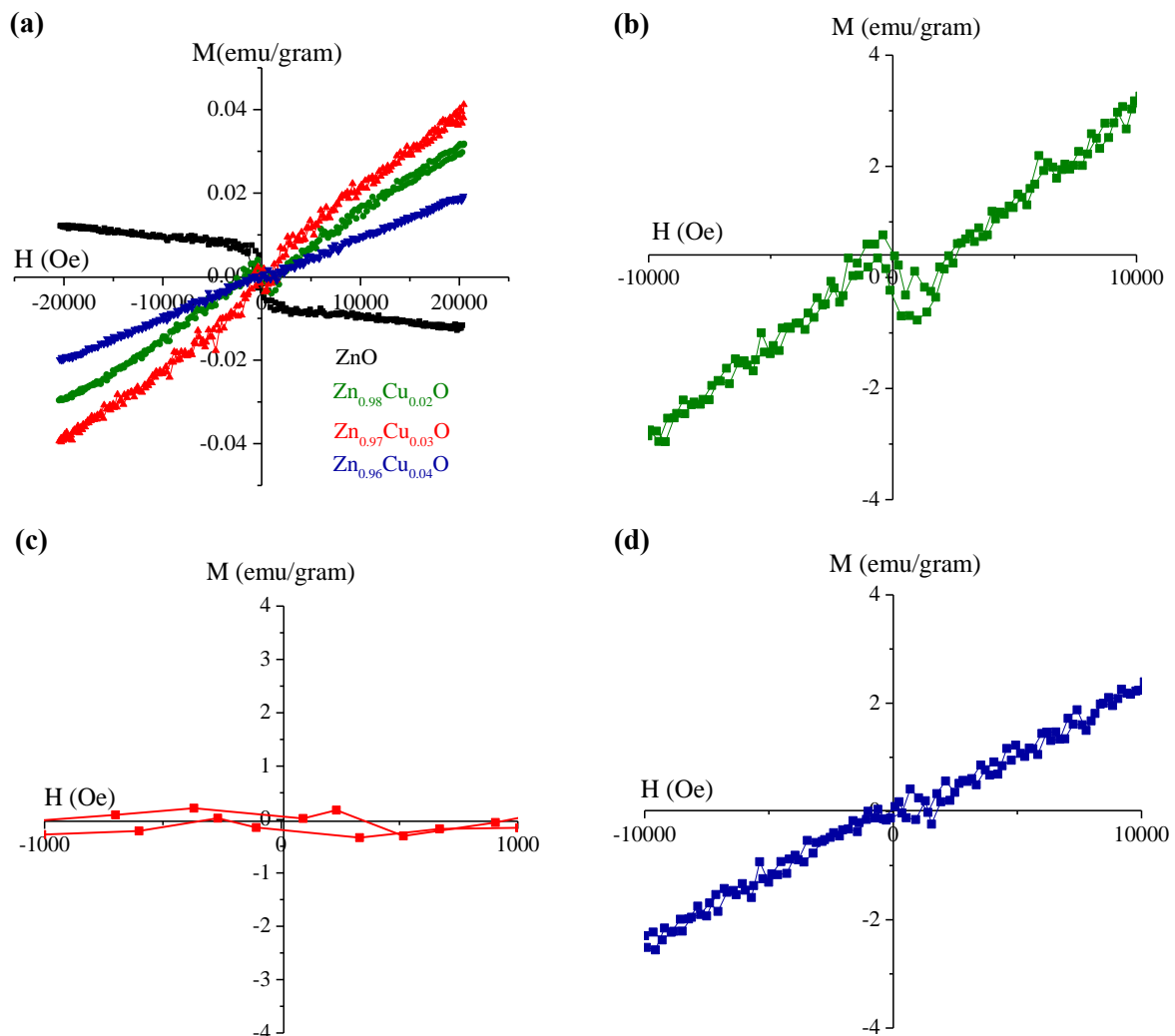


Figure 3. (a) The magnetic hysteresis loops of $\text{Zn}_{1-x}\text{Cu}_x\text{O}$ ($x = 0, 2, 3$ and 4 at%) samples at room temperature below 20 kOe, (b) The magnetic hysteresis loop of $\text{Zn}_{0.98}\text{Cu}_{0.02}\text{O}$, (c) The magnetic hysteresis loop of $\text{Zn}_{0.97}\text{Cu}_{0.03}\text{O}$ and (d) The magnetic hysteresis loop of $\text{Zn}_{0.96}\text{Cu}_{0.04}\text{O}$

4. Conclusion

$\text{Zn}_{1-x}\text{Cu}_x\text{O}$ ($x = 0, 2, 3$, and 4 at%) has been synthesized by using solid-state reaction, and their structures, electrical and magnetic properties were studied. Their XRD patterns showed that $\text{Zn}_{1-x}\text{Cu}_x\text{O}$ was polycrystalline with wurtzite hexagonal structure. The detailed XRD analysis indicated that some parts of Cu dopants substituted Zn on the $\text{Zn}_{1-x}\text{Cu}_x\text{O}$ system and some still in CuO form. The conductivity of $\text{Zn}_{1-x}\text{Cu}_x\text{O}$ was increased by increasing the dopant concentration. Crystal defects formed during the synthesis process of $\text{Zn}_{1-x}\text{Cu}_x\text{O}$ affected the capacitance and dielectric constant. $\text{Zn}_{1-x}\text{Cu}_x\text{O}$ became paramagnetic by increasing Cu dopants.

5. References

- [1] Ashokkumar M and Muthukumaran S 2014(a) *Journal of Magnetism and Magnetic Materials* **374** 61-66
- [2] Vojisavljević K, Žunić M, Branković G, Srećković T 2006 *Science of Sintering* **38** 131-138
- [3] Wang Z L 2004 *Journal of Physics Condensed Matter* **16** 829-858
- [4] Balamurugan S and Melba K 2014 *Journal of Nanoscience and Nanotechnology* **14** 1-9
- [5] Potzger K and Zhou S 2009 *Phys. Status Solidi B* **246** 1147-1167
- [6] Zheng J H, Song J L, Li X J, Jiang Q, and Lian J S 2011 *Cryst. Res. Technol* **46** 1143-1148
- [7] Owens F J. 2009 *Journal of Magnetism and Magnetic Materials* **321** 3734-3737
- [8] Wang Q, Wang J, Zhong X, Tan Q, Zhou Y 2012 *Solid State Communications* **152** 50-52.
- [9] Tseng Y W and Huang C L 2015 *Journal of Alloys and Compounds* **638** 29-33.
- [10] Ashokkumar M and Muthukumaran S 2014(b) *Optical Materials* **37** 671-678
- [11] Liu H, Yang J, Hua Z, Zhang Y, Yang L, Xiao L, Xie Z 2010 *Applied Surface Science* **256** 4162-4165
- [12] Karamat S, Rawat R S, Tan T L, Lee P, Springham S V, Rehman A, Chen R, Sun HD 2013 *J Supercond Nov Magn* **26** 187-195
- [13] Liu W, Tang X, Tang Z, Chu F, Zeng T, Tang N 2014 *Journal of Alloys and Compounds* **615** 740-744.
- [14] Zhao S, Bai Y, Chen J, Bai A and Gao W 2014 *Journal of Magnetism* **19** 68-71
- [15] Iqbal J, Safdar N, Jan T, Ismail M, Hussain S S, Mahmood A, Shahzad S, Mansoor Q 2014 *Journal of Materials Science & Technology* **437** 00215-1
- [16] Yildirim Ö A and Durucan C 2016 *Ceramics International* **42** 3229-3238
- [17] Hsu C L, Gao Y D, Chen Y S and Hsueh T J 2014 *Appl Mater Interfaces* **6** 4277-4285
- [18] Wan W, Huang J, Zhu L, Hu L, Wen Z, Sun L and Ye Z 2013 *Cryst Eng Comm* **15** 7887-7894.
- [19] Hu L, Zhu L, He H, Guo Y, Pan G, Jiang J, Jin Y, Sun L and Ye Z 2013 *Nanoscale* **5** 9577-9581
- [20] Fabbriyola S, Kennedy L J, Dakhel A A, Bououdina M, Vijaya J J, Ratnaji T 2016 *Journal of Molecular Structure* **1109** 89-96.
- [21] Giancoli D 2009 *Prentice Hall*. **658**. ISBN 0-13-149508-9.
- [22] Physical constants. Retrieved on 2011-12-17.
- [23] Kiesel P, Schmidt O, Geis A and Johnson N 2014 *Pramana-J. Phys* **X** 1-15
- [24] Mala N, Ravichandran K, Pandiarajan S, Srinivasan N, Ravikumar B, Pushpa K C S, Swaminathan K, Arun T 2016 *Ceramics International* **42** 7336-7346
- [25] Vachhani P S, Dalba G, Ramamoorthy R K, Rocca F, Sipr O and Bhatnagar A K *Journal Of Physics Condensed Matter* **24** 506001(1-7).

Acknowledgements

The authors are grateful to Laboratory of Advanced Magnetic Materials, Research Center for Physics-LIPI, Indonesia.